# Micropatterning of electrochemiluminescent polymers based on multipolar Ru-complex two-photon initiators

Rana Mhanna, Nicolas Durand, Paul Savel, Huriye Akdas-Kiliç, Stephania Abdallah, Davy-Louis Versace, Olivier Soppera, Jean-Luc Fillaut, Neso Sojic, Jean-Pierre Malval

# Micropatterning of electrochemiluminescent polymers based on multipolar Ru-complex two-photon initiators

**Rana Mhanna [a], Nicolas Durand [b], Paul Savel [b], Huriye Akdas-Kiliç [bc], Stephania Abdallah [a], Davy-Louis Versace [d], Olivier Soppera [a], Jean-Luc Fillaut [b], Neso Sojic [e] and Jean-Pierre Malval [a]***

[a]

[a]*Institut de Science des Matériaux de Mulhouse CNRS-UMR 7361, Université de Haute Alsace, Mulhouse, France. E-mail: jean-pierre.malval@uha.fr*

[b]*Université de Rennes, Institut des Sciences Chimiques de Rennes CNRS UMR, Rennes, France*

[c]*Yildiz Technical University, Department of Chemistry, Istanbul, Turkey*

[d]*Institut de Chimie et des Matériaux Paris-Est, UMR-CNRS 7182, Université Paris-Est Créteil, Thiais, France*

[e]*Université de Bordeaux, Institut des Sciences Moléculaires, UMR 5255 CNRS, Talence, France*

## Abstract

In this work, we present an original stereolithography strategy based on multibranched Ru-complexes with a high two-photon initiating ability allowing the 'one-pot' direct laser writing of ECL-active materials deposited onto electro-active surfaces at the µm scale.

Two-photon polymerization (2PP) has emerged as one of the most efficient maskless stereolithography technologies.[1,2] Such a direct laser writing method allows the fabrication of intricate 3D-structures with a spatial resolution down to the sub-µm scale.[3] 2PP technology, which is now commercially available, has been largely dedicated to the photopatterning of advanced functional materials with a plethora of applications such as

photonic metamaterials, stimuli responsive devices, microelectromechanical systems or micromedicine.[1-4] The unique capability of 2PP relies on its diffraction unlimited spatial confinement due to the non-linear absorption of the initiator component, which is photoactivated at the focus point of a tightly focalized *fs*-pulse laser. In this context, the photoinitiator clearly has a pivotal role and should both exhibit a high two-photon absorption (2PA) cross section as well as an efficient quantum yield for the generation of reactive species that promote monomer cross-linking.[5] Contrary to the very large majority of 2PA initiators whose reactivity mainly relies on their hydrogen abstraction ability[6] for free radical generation, very few examples depicting direct two-photon cleavable systems have been reported to date.[7] This contribution precisely presents one of these unusual examples corresponding to two π-conjugated ruthenium-based complexes with electrochemilumiscence (ECL[8]) (Scheme 1), which not only displays a sizeable 2PA cross section in the NIR range but also presents an intrinsic photoinitiation reactivity when directly associated with acrylate-based monomers. In addition, we demonstrate a covalent integration of the Ru-complex within the polymer matrix implementing for the first time an original ECL functionality[8,9] into the two-photon patterned materials.

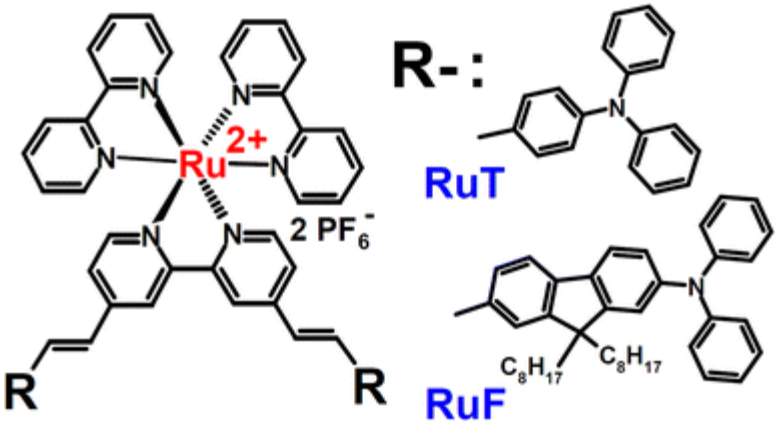


**Scheme 1** Molecular structures of the Ru-complexes.

Fig. 1 shows the one- (1PA) and two-photon (2PA) absorption spectra of the complexes in acetonitrile (ACN). As described previously,[10] these Ru-complexes exhibit significant 2PA cross sections (σ) in the NIR region with $\sigma_{MAX}$ of about 312 ± 47 GM for **RuT** and 597 ± 90 GM for **RuF**. Note that these 2PA cross sections are more than one order of magnitude higher than that measured for $Ru(bpy)_3^{2+}$ ($\sigma_{MAX}$ ~ 12 ± 2 GM[11]). As shown in Fig. 1, both complexes display similar 2PA spectra with two distinctive bands at $\sigma_{MAX}$ ~ 850 nm and ~980 nm, which, respectively, correspond to the intraligand charge transfer transition (ILCT) and to a metal-

ligand charge-transfer (MLCT) one. These transitions both imply a long range electronic delocalization along the quadrupolar π-conjugated bipyridine, which is mainly responsible for the observed 2PA enhancement. In the same manner, the presence of such a multibranched bipyridine strongly affects the luminescence properties of the Ru-complexes as compared to that of $Ru(bpy)_3^{2+}$. Indeed, both complexes display a similar phosphorescent spectrum with $\lambda_{MAX}$ at ~ 700 nm, which positions their triplet state energy below that of $Ru(bpy)_3^{2+}$ ($\Delta E_T$ ~ 0.2 eV, see Fig. S1 and Table S1, ESI). Such a significant energy gap underlines that the emissive $^3$MLCT states of the complexes exhibit a distinctive electronic configuration as compared to that of $Ru(bpy)_3^{2+}$ with an excitation localized within the multibranched bipyridine ligand. This electronic configuration should be responsible for the intrinsic photoinitiating reactivity of these Ru-complexes as described hereafter. The redox and ECL properties of the Ru-complexes were investigated in ACN. Fig. 2A and Fig. S2A (ESI), respectively, depict the cyclic voltammograms (CV) of **RuF** and **RuT**. Their corresponding ECL-voltage curves (Fig. 2B and Fig. S2B, ESI) were recorded in the presence of a large excess of tri-*n*-propylamine (**TrPA**) used as an anodic sacrificial co-reactant. Note that the ECL signals result from an oxidative-reductive sequence[13] in which the oxidized species of the metal-complex and **TPrA** are both generated in the vicinity of the working electrode. The radical cation of **TrPA** is known to undergo a subsequent deprotonation[14] with the formation of a neutral radical (**TPrA**$^{\bullet}$), which can readily reduce the oxidized species of the Ru-complexes. These electrogenerated intermediates can recombine with each other through an electron transfer (eT) reaction yielding the Ru-complex in its excited state that deactivates radiatively. For **RuF**, the anodic region of CV clearly displays two quasi-reversible oxidation waves with redox potentials at 0.47 V and 0.86 V *vs.* $Fc/Fc^+$. These CVs reasonably correspond to those observed for the branched bipyridine ligand and $Ru(bpy)_3^{2+}$, respectively (see Fig. S3, ESI†). Interestingly, the peak current of the first oxidation wave is approximately twice higher than that of the second one suggesting a two-electron oxidation process that involves the two external arylamine groups of **RuF**. These two equivalent electrophores seem activated at very close oxidation potentials presumably due to the large distance separating these two redox centers and also due to a weak electronic communication between each π-conjugated branch.[12] Such an electrochemical equivalence

is also corroborated by a single ECL peak whose maximum intensity at 0.49 V *vs.* $Fc/Fc^+$ matches the first oxidation potential of **RuF**.

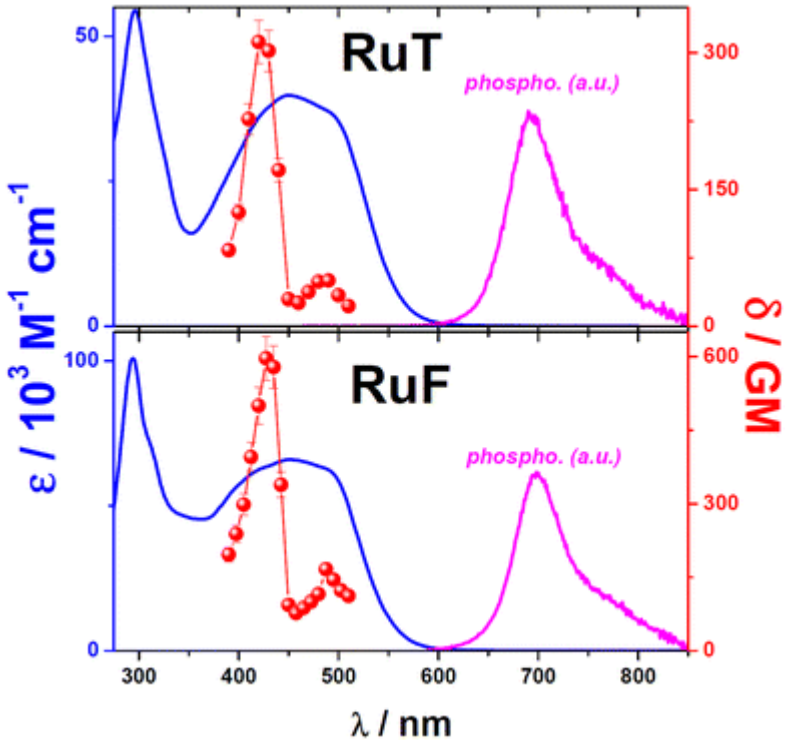


**Fig. 1** 1PA (blue lines), 2PA (circles) and luminescence spectra of **RuT** and **RuF** in ACN. The 2PA spectrum
laser excitation wavelength.

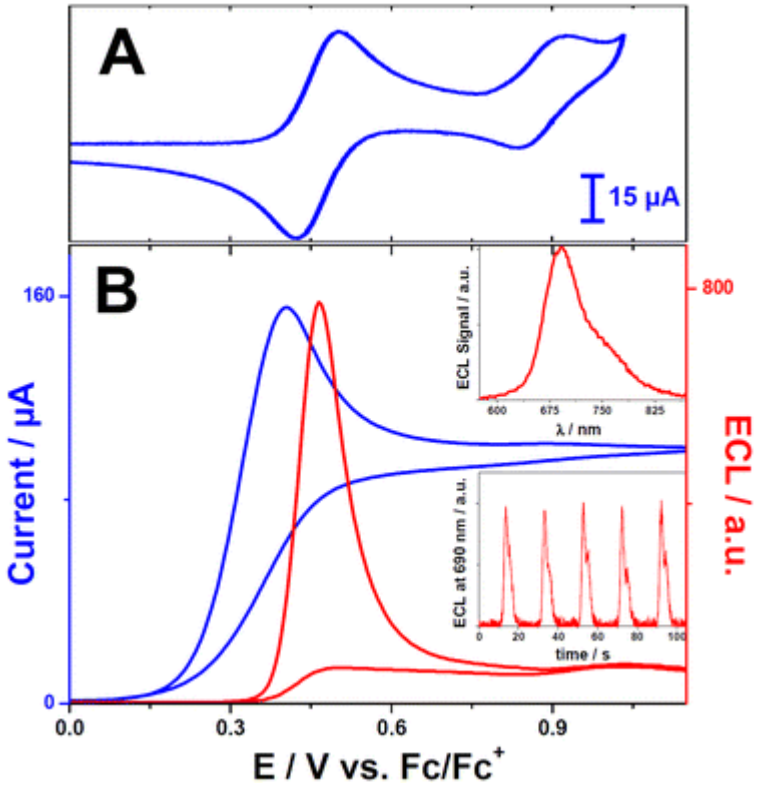


**Fig. 2** (A) CV of **RuF** (1.1 mM) in ACN on a platinum electrode (0.1 M $TBAPF_6$, 100 mV $s^{-1}$). (B) CV and in the presence of **TPrA** (50 mM) on a screen-printed gold electrode (0.1 M $TBAPF_6$, 50 mV $s^{-1}$). Insets: presence of **TPrA** at 0.49 V *vs.* $Fc/Fc^+$. OFF-ON of the ECL periodic signal recorded at 690 nm during 5 cycle 0.2 and 0.6 V.

By contrast, the length decrease of the arylamine branches on going from **RuF** to **RuT** disrupts such an electrochemical equivalence and gives rise to two anodic waves (0.57 V and 0.64 V *vs.* $Fc/Fc^+$) that echo two consecutive ECL peaks observed within the same potential range as shown in Fig. S2B (ESI†). Therefore, it can be derived that both complexes display ECL signals, which mainly proceed through the exergonic reduction of their arylamine-centred radical cations. It should also be underlined that the ECL-spectrum of each complex perfectly matches its corresponding phosphorescence band (see insets in Fig. 2B and Fig. S2B, ESI). In addition to these 2PA and ECL properties, **RuT** and **RuF** also exhibit an interesting photoinitiation reactivity for free radical polymerization. To demonstrate this reactivity, each Ru-complex was mixed with a viscous pentaerythritol triacrylate resin (**PETIA**, see Scheme S1, ESI). The photoinitiation reaction was then monitored by epiluminescence microscopy upon visible irradiation of a drop of each formulation using a 40×, 0.65-NA objective. Fig. 3 and Fig. S3 (ESI), respectively, show the

evolution of the luminescence and the absorption spectra of **RuF** in the resin during its irradiation. Similar measurements are presented in Fig. S6 (ESI) for **RuT**.

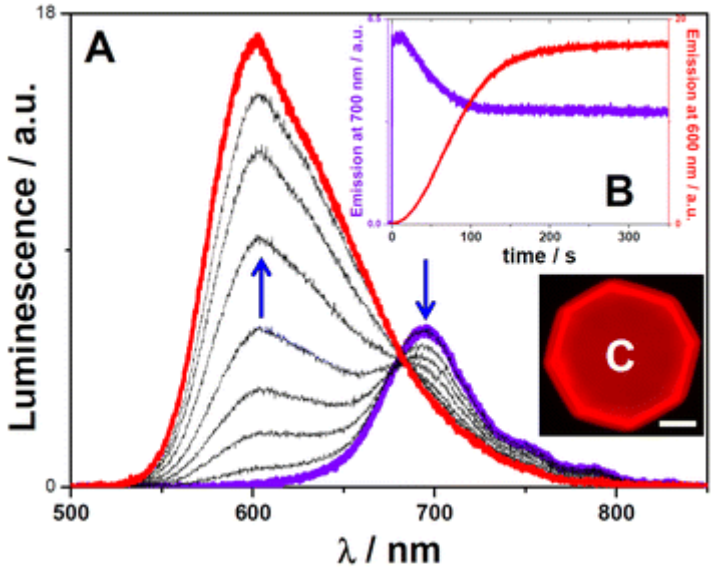


**Fig. 3** (A) Evolution of the luminescence spectrum of **RuF** (0.3 wt%) in triacrylate resin irradiated under a m μW). (B) Time-dependent changes of the luminescence signal recorded at 600 nm and 700 nm. (C) Epilumine photopolymerized octagonal microdot (scale bar: 20 μm).

Interestingly, both complexes behave in the same manner. Their luminescence spectra disappear concomitantly with the growth of a new band that perfectly matches that of $Ru(bpy)_3^{2+}$ (see Fig. S7, ESI). In the same manner, the longest wavelength absorption band of each complex collapses resulting in the appearance of the MLCT band of $Ru(bpy)_3^{2+}$ (Fig. S5 and inset Fig. S6, ESI). Note that the observed photoreactions are quantitative since the excitation spectra of the generated by-products match their corresponding final absorption spectra. Moreover these photoreactions only occur in the presence of acrylate-based resins and cannot be observed for instance in viscous glycerol using the same conditions. Finally, the irradiation of the formulation rapidly generates an emissive photopolymerized microdot, which has been isolated by rinsing away the unexposed monomers as typically illustrated in Fig. 3C for **RuF**. All these spectral changes clearly indicate that the polymerization reaction proceeds through a photoinitiation step, which affects the integrity of the complexes by disrupting the π-conjugation of their multibranched bipyridine ligands. Such a disruption should specifically concern the 2-(4-vinyl) pyridine moieties whose olefinic bond is known to be photochemically unstable and prone to C=C breaking with

concomitant dimerization or Michael addition reactions.[15] In our e, the photoinitiation step should presumably stem from a direct addition of **RuF** or **RuT** onto a double bond of the triacrylate monomer consecutively to the olefinic bond breaking at the $^3$MLCT state. This mechanism at the excited triplet state is also in line with the presence of isoemissive points at 685 nm for **RuT** and 681 nm for **RuF**, which suggests the occurrence of a photochemical reaction at the triplet state manifold. Of particular interest, this one-photon polymerization reaction can be perfectly extended to a two-photon activation process. For instance, Fig. 4 and Fig. S8 (ESI†) show different scanning electron microscopy (SEM) micrographs of microstructures with arbitrary geometries, which were two-photon fabricated at 800 nm using the previous resins. In Fig. 4 for instance, the µ-object consists in nine entangled circles of 50 µm diameter and 3 µm thick.

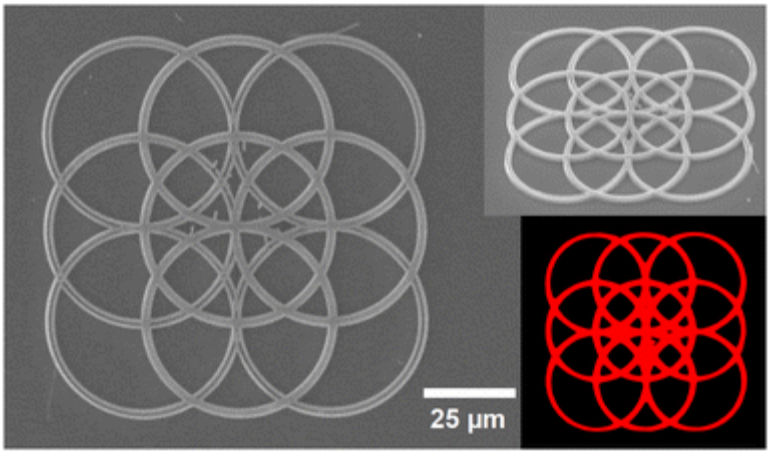


**Fig. 4** SEM micrographs of a two-photon polymerized 2D microstructure with its corresponding epilumines

The µ-structure exhibits the same luminescent fingerprint as that observed after one photon polymerization. Such an equivalency clearly generalizes the initiation mechanism, which should promote a covalent integration of the $Ru(bpy)_3^{2+}$ subunits into the photopatterned materials. In order to demonstrate this grafting effect, we have prepared similar acrylate formulations as previously described but with the incorporation of 70 wt% of a poly(ethyleneglycol)diacrylate monomer (**PEGDA**, see Scheme S1, ESI†). As a result, the corresponding photopolymers become permeable to ACN and allow mass transport of embedded species when incubated into an imbibing solvent. Using the new formulation with **RuF**, Fig. S9 (ESI) shows a polymerized microdot whose radius is typically multiplied by a factor ~1.2 when immersed in ACN. This swelling effect corroborates the solvent uptake

process due to the permeability of the polymer. Moreover, the luminescence signal recorded from the microdot remains perfectly invariant during 20 min incubation in ACN, which excludes any dyes leaking from the microstructure. This demonstrates a covalent grafting of the emissive $Ru(bpy)_3^{2+}$ by-products within the matrix. The same properties can also be derived from the **RuT** formulation (see Fig. S10, ESI). As a comparative example, we also fabricated a similar microdot based on a bi-component system using the same monomers but associating $Ru(bpy)_3^{2+}$ as a photosensitizer with an aliphatic amine as a co-initiator (*i.e.* the *N*-methyl diethanol amine). Fig. S11 (ESI) illustrates the time-dependent decrease of the luminescence from this microdot when incubated in ACN. In parallel, the surrounding solvent becomes luminescent indicating an important leaking of the photosensitizer from the incubated object (inset Fig. S11, ESI). This leaking effect underlines the crucial role of the π-conjugated branches of our complexes for their subsequent light-triggered grafting within the polymer structure. Interestingly, the permeability of the photopolymer also authorizes to probe the ECL ability of the $Ru(bpy)_3^{2+}$ centers. In this respect, several microstructures (*i.e.* µ-grids) were two-photon patterned at the surface of a screen-printed gold electrode as depicted in Fig. 5 and Fig. S12 (ESI†) for **RuF** and **RuT,** respectively. Each µ-grid consists in periodic 20 × 20 µm squares of 3.1 ± 0.5 µm thick. For **RuF**, Fig. 5C both displays the CV and the ECL profile of the sample in the presence of **TPrA** in ACN. By scanning the potential up to 1.09 V, the ECL signal clearly increases with a maximum at 0.87 V *vs.* $Fc/Fc^+$. This potential, significantly higher than that of the oxidation of **TPrA** ($E_{ox}$ ~ 0.40 V in CV), should be ascribed to the oxidative activation of the $Ru(bpy)_3^{2+}$ centers, which is subsequently responsible for the ECL generation. This effect agrees with the recorded ECL-spectra in Fig. 5D, which coincide with the luminescence of Ru-based by-products generated during the two-photon fabrication step. Note that the same ECL behaviour can be derived with µ-grids generated with **RuT** formulation (Fig S12, ESI†), which generalizes our cross coupling demonstration between 2PA stereolithography and the ECL properties.

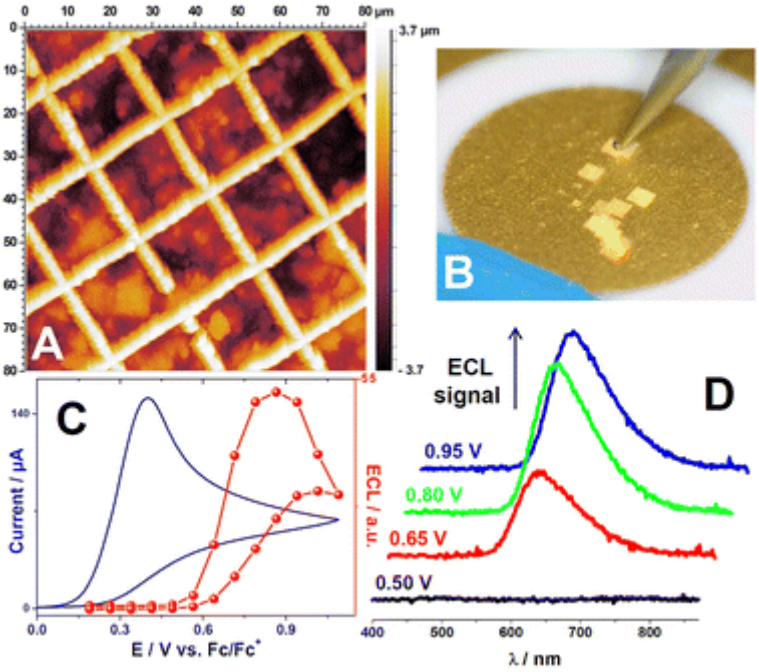


**Fig. 5** (A) AFM image of a two-photon polymerized µ-grid fabricated on a screen-printed gold electrode. (B electrode with various µ-grids. (C) CV and ECL signal of the µ-grids in ACN in the presence of **TPrA** (50 s$^{-1}$). (D) ECL-spectrum as a function of the applied potential.

In conclusion, we have developed a multiphoton fabrication strategy based on highly two-photon active Ru-complex initiators. This simple 'one-pot' processing method allows the 2D-patterning of ECL-active materials directly integrated onto electro-active surfaces at the µm-scale. This general approach that judiciously combines two-photon stereolithography and ECL systems clearly paves the way to the future development of new miniaturized ECL-based microsensors and devices.[9]

## Notes and references


1. C. Barner-Kowollik, M. Bastmeyer, E. Blasco, G. Delaittre, P. Müller, B. Richter and M. Wegener, *Angew. Chem., Int. Ed.*, 2017, **56**, 15828–15845 .
2. C. N. LaFratta, J. T. Fourkas, T. Baldacchini and R. A. Farrer, *Angew. Chem., Int. Ed.*, 2007, **46**, 6238–6258 .
3. L. Li, R. R. Gattass, E. Gershgoren, H. Hwang and J. T. Fourkas, *Science*, 2009, **324**, 910–913 .
4. (*a*) G. Kenanakis, A. Xomalis, A. Selimis, M. Vamvakaki, M. Farsari, M. Kafesaki, C. M. Soukoulis and E. N. Economou, *ACS Photonics*, 2015, **2**, 287–294 ; (*b*) J. Torgersen, X.-H. Qin, Z. Li, A. Ovsianikov, R. Liska and J. Stampfl, *Adv. Funct. Mater.*, 2013, **23**, 4542–4554 ; (*c*) S. Ushiba, S. Shoji, K. Masui, J. Kono and S. Kawata, *Adv. Mater.*, 2014, **26**, 5653–5657 ; (*d*) M. Lunzer, L. Shi, O. G. Andriotis, P. Gruber, M. Markovic, P. J. Thurner, D. Ossipov, R. Liska and A. Ovsianikov, *Angew. Chem., Int. Ed.*, 2018, **57**, 15122–15127 ;

(*e*) Y.-L. Sun, W.-F. Dong, R.-Z. Yang, X. Meng, L. Zhang, Q.-D. Chen and H.-B. Sun, *Angew. Chem., Int. Ed.*, 2012, **51**, 1558–1562 .
5. K.-S. Lee, D.-Y. Yang, S. H. Park and R. H. Kim, *Polym. Adv. Technol.*, 2006, **17**, 72–82 .
6. (*a*) R. Nazir, P. Danilevicius, A. I. Ciuciu, M. Chatzinikolaidou, D. Gray, L. Flamigni, M. Farsari and D. T. Gryko, *Chem. Mater.*, 2014, **26**, 3175–3184 ; (*b*) Z. Li, N. Pucher, K. Cicha, J. Torgersen, S. C. Ligon, A. Ajami, W. Husinsky, A. Rosspeintner, E. Vauthey, S. Naumov, T. Scherzer, J. Stampfl and R. Liska, *Macromolecules*, 2013, **46**, 352–361 ; (*c*) R. Nazir, E. Balciunas, D. Buczynska, F. Bourquard, D. Kowalska, D. Gray, S. Mackowski, M. Farsari and D. T. Gryko, *Macromolecules*, 2015, **48**, 2466–2472 .
7. (*a*) R. Zhou, J.-P. Malval, M. Jin, A. Spangenberg, H. Pan, D. Wan, F. Morlet-Savary and S. Knopf, *Chem. Commun.*, 2019, **55**, 6233–6236 ; (*b*) P. Hu, W. Qiu, S. Naumov, T. Scherzer, Z. Hu, Q. Chen, W. Knolle and Z. Li, *ChemPhotoChem*, 2020, **4**, 224–232 ; (*c*) W. Qiu, P. Hu, J. Zhu, R. Liu, Z. Li, Z. Hu, Q. Chen, K. Dietliker and R. Liska, *ChemPhotoChem*, 2019, **3**, 1090–1094 ; (*d*) R. Nazir, P. Danilevicius, D. Gray, M. Farsari and D. T. Gryko, *Macromolecules*, 2013, **46**, 7239–7244 .
8. C. Ma, Y. Cao, X. Gou and J.-J. Zhu, *Anal. Chem.*, 2020, **92**, 431–454 .
9. X. Ma, W. Gao, F. Du, F. Yuan, J. Yu, Y. Guan, N. Sojic and G. Xu, *Acc. Chem. Res.*, 2021, **54**, 2936–2945 .
10. N. Durand, R. Mhanna, P. Savel, H. Akdas-Kilig, J.-P. Malval, O. Soppera and J.-L. Fillaut, *Chem. Commun.*, 2020, **56**, 12801–12804 .
11. C. W. Stark, A. Trummal, M. Uudsemaa, J. Pahapill, M. Rammo, K. Petritsenko, M.-M. Sildoja and A. Rebane, *Commun. Chem.*, 2019, **2**, 108 .
12. D. H. Evans, *Chem. Rev.*, 2008, **108**, 2113–2144 .
13. Z. Liu, W. Qi and G. Xu, *Chem. Soc. Rev.*, 2015, **44**, 3117–3142 .
14. W. Miao, J.-P. Choi and A. J. Bard, *J. Am. Chem. Soc.*, 2002, **124**, 14478–14485 .
15. (*a*) S. Bradamante, A. Facchetti and G. A. Pagani, *J. Phys. Org. Chem.*, 1997, **10**, 514–524 ; (*b*) R. Kannan, G. S. He, L. Yuan, F. Xu, P. N. Prasad, A. G. Dombroskie, B. A. Reinhardt, J. W. Baur, R. A. Vaia and L.-S. Tan, *Chem. Mater.*, 2001, **13**, 1896–1904 .